Non-resonant and Resonant X-ray Scattering Studies on Multiferroic $TbMn_2O_5$

J. Koo[1], C. Song[1], S. Ji[1], J.-S. Lee[1], J. Park[1], T.-H. Jang[1], C.-H. Yang[1], J.-H. Park[1,2], Y. H. Jeong[1], K.-B. Lee[1,2],*
T.Y. Koo[2], Y.J. Park[2], J.-Y. Kim[2], D. Wermeille[3],† A.I. Goldman[3], G. Srajer[4], S. Park[5], and S.-W. Cheong[5,6]
[1] *eSSC and Department of Physics, POSTECH, Pohang 790-784, Korea*
[2] *Pohang Accelerator Laboratory, Pohang University of Science and Technology, Pohang 790-784, Korea*
[3] *Ames Laboratory, Department of Physics and Astronomy, Iowa State University, Ames, IA 50011, USA*
[4] *Advanced Photon Source, Argonne National Laboratory, Argonne, IL 60439, USA*
[5] *Rutgers Center for Emergent Materials and Department of Physics and Astronomy, Rutgers University, Piscataway, NJ 08854, USA*
[6] *Laboratory of Pohang Emergent Materials and Department of Physics, POSTECH, Pohang 790-784, Korea*

(Dated: February 1, 2008)

Comprehensive x-ray scattering studies, including resonant scattering at Mn *L*-edge, Tb *L*- and *M*-edges, were performed on single crystals of $TbMn_2O_5$. X-ray intensities were observed at a forbidden Bragg position in the ferroelectric phases, in addition to the lattice and the magnetic modulation peaks. Temperature dependences of their intensities and the relation between the modulation wave vectors provide direct evidences of exchange striction induced ferroelectricity. Resonant x-ray scattering results demonstrate the presence of multiple magnetic orders by exhibiting their different temperature dependences. The commensurate-to-incommensurate phase transition around 24 K is attributed to discommensuration through phase slipping of the magnetic orders in spin frustrated geometries. We proposed that the low temperature incommensurate phase consists of the commensurate magnetic domains separated by anti-phase domain walls which reduce spontaneous polarizations abruptly at the transition.

PACS numbers: 77.80.e-, 75.25.+z, 64.70.Rh, 61.10.-i

In recent years, much attention has been paid to multiferroic materials, in which magnetic and ferroelectric orders coexist and are cross-correlated [1, 2, 3, 4, 5, 6, 7, 8, 9, 10], due to theoretical interests and potential application to magnetoelectric (ME) devices. Manipulation of electric polarizations by external magnetic fields has been demonstrated in some of these materials [4, 5]. Orthorhombic $TbMn_2O_5$, one of the multiferroic materials, displays a rich phase diagram. Upon cooling through $T_N \sim 41$ K, $TbMn_2O_5$ becomes antiferromagnetic with an incommensurate magnetic (ICM) order which transits to a commensurate magnetic (CM) phase with spontaneous electric polarization at $T_{c1} \sim 36$ K, and reenters a low temperature incommensurate magnetic (LT-ICM) phase at $T_{c2} \sim 24$ K. Anomalies of ferroelectricity and dielectric properties were observed concurrently with these magnetic phase transitions [4, 9]. Especially, the reentrant LT-ICM phase is a phenomenon peculiar to $R\mathrm{Mn_2O_5}$ multiferroics while commensurate phases are more common as the low temperature ground states. Since the CM to LT-ICM phase transition is also accompanied with an abrupt loss of spontaneous polarizations, it is critical to elucidate the natures of the incommensurability of the material, including the mechanism of the CM to LT-ICM phase transition.

The origin of the complex phases of the material is attributed to the coupling between magnetic moments of Mn ions and lattice [8, 9]. It is suggested that, when a magnetic order is modulated with a wave vector $\boldsymbol{q}_m$, the exchange striction affects inter-atomic bondings resulting in a periodic lattice modulation with a wave vector $\boldsymbol{q}_c = 2\boldsymbol{q}_m$ [5, 6, 7, 8, 9]. Recently, Chapon *et al.* proposed for $R\mathrm{Mn_2O_5}$ systems that ferroelectricity results from the exchange striction of acentric spin density waves for the CM phases [9]. Indeed, Kimura *et al.* insisted that CM modulations are indispensable to the ferroelectricity in the LT-ICM phase, from their neutron scattering results on $HoMn_2O_5$ under high magnetic fields [11]. However, lattice distortions derived from ICM spin structures turned out to describe well the spontaneous polarizations of YMn_2O_5 even in the ICM phase [12], implying that commensurability is not a necessary condition for the ferroelectricity. In order to understand the intriguing magnetoelectricity well, detailed information on the lattice and spin structure changes is necessary. However, only limited crystallographic data are available and even any direct evidence on the symmetry lowering has not been reported yet [9, 10, 11, 12, 13, 14].

In this letter, we present synchrotron x-ray scattering results on single crystals of $TbMn_2O_5$. Since x-ray scattering is sensitive to both lattice and magnetic modulations, x-ray scattering with intense undulator x-rays allowed simultaneous measurements for $\boldsymbol{q}_m$ and $\boldsymbol{q}_c$. Non-resonant x-ray scattering results show the relationship of $\boldsymbol{q}_c = 2\boldsymbol{q}_m$, confirming lattice modulations are generated by the magnetic orders. A (3 0 0) forbidden Bragg peak, which is a direct evidence of the symmetry lowering to a non-centrosymmetry space group, was observed in the ferroelectric (FE) phases. Furthermore, the temperature dependence of the peak intensity, $I_{(300)}$, was found to coincide with those of the lattice modulation peak intensities, I_c, and the spontaneous polarization square,P^2, in

the CM phase. This indicates the ferroelectricity is generated by the lattice modulations. In the LT-ICM phase, temperature dependences of I_c cannot be described by a single order parameter, implying the presence of different magnetic orders. Resonant x-ray magnetic scattering results at Mn L-, Tb L_3- and M_5-edges show that each magnetic order has its own temperature dependence. It is proposed that CM to LT-ICM phase transition is induced by discommensuration through phase slipping due to competing magnetic orders under the frustrated geometry. Moreover, the CM modulations with anti-phase domain walls are consistent with the temperature dependences of $\boldsymbol{q}_m$ and $I_{(300)}$ in the LT-ICM phase, and explain well the abrupt loss of P at the transition.

Single crystals of $TbMn_2O_5$ were grown by a flux method [4]. The specimen used for the hard x-ray scattering measurements has a plate-like shape with (1 1 0) as a surface normal direction. Its mosaicity was measured to be about 0.01° at (3 3 0) Bragg reflection. For soft x-ray scattering, a different sample was cut and polished to have (2 0 1) as a surface normal direction. Soft x-ray scattering measurements were performed at 2A beamline in the Pohang Light Source (PLS). Details of the soft x-ray scattering chamber were described elsewhere [15]. X-ray diffraction experiments were conducted at the 3C2 bending magnet beamline in the PLS and at the 6-ID undulator beamline in the Midwest Universities Collaborative Access Team (MUCAT) Sector in the Advanced Photon Source. For non-resonant x-ray scattering experiments, 6.45 keV was selected as an incident x-ray energy below Mn K-edge ($\sim$ 6.55 keV). All the incident x-rays were σ-polarized and PG(006) was used to have a σ-to-π channel at Tb L_3-edge.

Nonresonant x-ray scattering measurements were performed to investigate the temperature dependence of $\boldsymbol{q}_m$ and $\boldsymbol{q}_c$ simultaneously. The measured lattice modulation peak position of (2 5 -0.5) for the CM phase and those of its 4 split peaks for the ICM phases are presented as solid and open circles, respectively, in Fig. 1 (a). For magnetic satellites, (2.5 5 -0.25) peak and its 2 split ones were measured for the CM and ICM phases. Their positions are presented as solid and open squares, respectively. The magnetic and lattice modulation satellites for ICM phases are linked with broken and solid lines to their corresponding main Bragg peaks. Temperature dependences of $\boldsymbol{q}_m$ and $\boldsymbol{q}_c$ are shown in Fig. 1 (b) and (c). From the results, it is obvious that relation, $\boldsymbol{q}_c = 2\boldsymbol{q}_m$, holds within experimental errors in the whole temperature range below T_N. It is consistent with the magnetic order induced lattice modulations. The temperature dependence of $\boldsymbol{q}_m$ shown here is qualitatively similar to the neutron scattering results by others [16]. Below T_N, ICM magnetic peaks develop, and $\boldsymbol{q}_m$ locks into a CM ordering at ($\frac{1}{2}$ 0 $\frac{1}{4}$) via a first order transition at T_{c1}. On further cooling the sample below T_{c2}, the CM to LT-ICM phase transition takes place. With

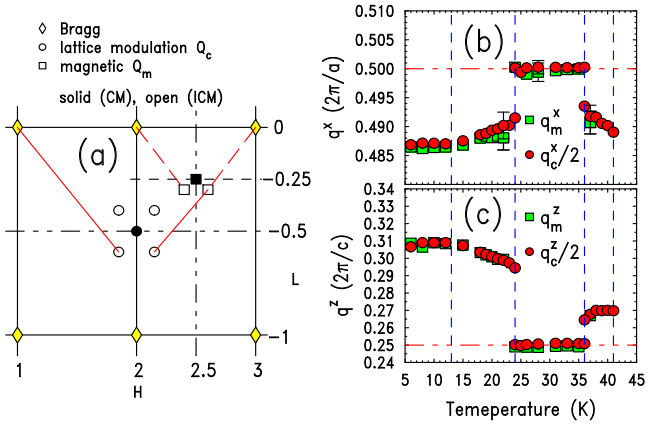

FIG. 1: (Color online) Positions of the measured magnetic satellites (square) and lattice modulation peaks (circle) in the (h 5 l) reciprocal lattice plane are shown in (a). The temperature dependences of q_m^x (square) and q_c^x (circle), and those of q_m^z (square) and q_c^z (circle) are shown in (b) and (c), respectively. For direct comparisons with those of $\boldsymbol{q}_m$, the components of $\boldsymbol{q}_c$ are divided by two. Vertical broken lines indicate $T_N \sim 41$ K, $T_{c1} \sim 36$ K, $T_{c2} \sim 24$ K and $T_{c3} \sim 13$ K, respectively.

further decreasing temperature, $\boldsymbol{q}_m$ of the LT-ICM modulations evolves and is eventually pinned around (0.486 0 0.308) which can be approximated to a CM value of ($\frac{17}{35}$ 0 $\frac{4}{13}$) at $T_{c3} \sim 13$ K. Such a long-period CM modulation can be interpreted as the CM modulations ($\boldsymbol{q}_m = (\frac{1}{2}\ 0\ \frac{1}{4})$) with domain walls, as is the case for $ErNi_2B_2C$ [17].

As shown in Fig. 2 (a), measurable x-ray intensities were observed, in the ferroelectric phase, at (3 0 0) Bragg position which is forbidden under a space group of the room temperature paraelectric phase, $Pbam$. Residual intensities above T_{c1} are due to higher harmonic

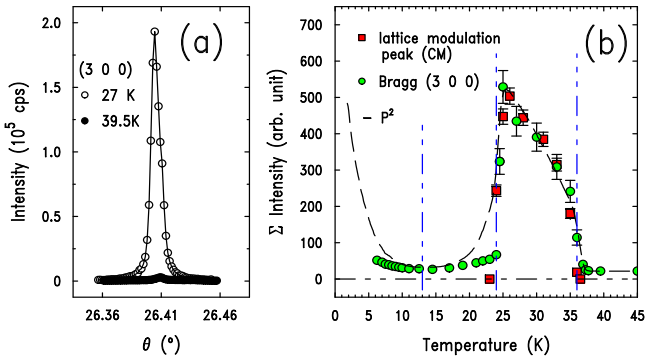

FIG. 2: (Color online) (a) Rocking curves of a (3 0 0) forbidden Bragg peak measured below (open) and above T_{c1} (solid). (b) Temperature dependences of the integrated intensities of a (3 0 0) Bragg peak (circle), CM lattice modulation peak (square) and squared spontaneous polarization (broken line) taken from Ref. 4. All the data are properly scaled.

contaminations. Values for full-width-at-half-maximum (FWHM) of the peak are about 0.01°, close to those of (4 0 0) main Bragg peak in the LT-ICM phase. The results explicitly evidenced that inversion symmetry is broken concomitantly with the FE phase as speculated before. According to the models suggested by others [9, 10], displacements of Mn^{3+} are in ab-plane. While b-axis components of the atomic displacements mainly contribute to P, a-axis components enable the emergence of $I_{(300)}$. If the atomic displacements correspond to the periodic lattice modulations, it is expected that both P^2 and $I_{(300)}$ are proportional to I_c, as shown in Fig. 2 (b). (The spontaneous polarization data are taken from Ref. 4 and are shifted in order to get the same values for T_{c1}.) It confirms that spontaneous polarization is due to the atomic displacements driven by magnetic orders: a direct crystallographic evidence of exchange striction as the origin of ferroelectricity in the material [8, 9, 10, 12]. Also it is noted that $I_{(300)}$ drops abruptly at T_{c2} and has a broad minimum around T_{c3}.

Though many interesting ME phenomena have been reported in the LT-ICM phases below T_{c2} [4, 11, 18, 19], their basic mechanisms still remain to be understood. Since the lattice modulations reflect basic ME natures, temperature dependences below T_{c2} of integrated intensities were measured at the four split ICM peak positions illustrated in Fig. 1 (a). From the results displayed in Fig. 3, it is clear that temperature dependences of all four peaks cannot be described by a single order parameter, implying the presence of various magnetic orders having the same $\boldsymbol{q}_m$'s but different temperature dependences.

To investigate different magnetic orders, we performed resonant x-ray magnetic scattering measurements at Mn L-, Tb L_3- and M_5-edges. Figure 4 (a) shows energy profiles around Mn L-edge of magnetic satellites at 10 K and x-ray absorption spectroscopy (XAS) at room temperature. Magnetic peaks and XAS data clearly show resonances at both Mn L_2- and L_3-edges. XAS results show broad peaks containing contributions from the multiplet states of $3d$ electrons of Mn^{3+} and Mn^{4+} ions. Magnetic satellites show relatively sharp double peaks at both Mn L-edges. The sharp resonances represent different multiplet states of Mn $3d$ electrons including charge transfer excitations, while Mn ions are expected to be in the high-spin configurations with all the $3d$ electron spins aligned

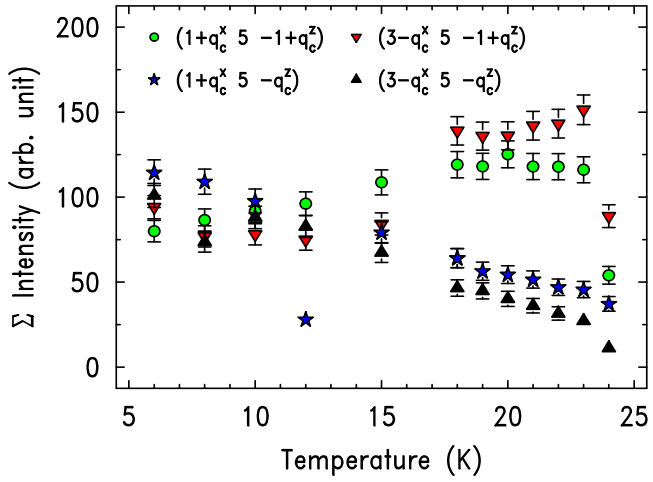

FIG. 3: (Color online) Temperature dependences of the ICM lattice modulation peak intensities.

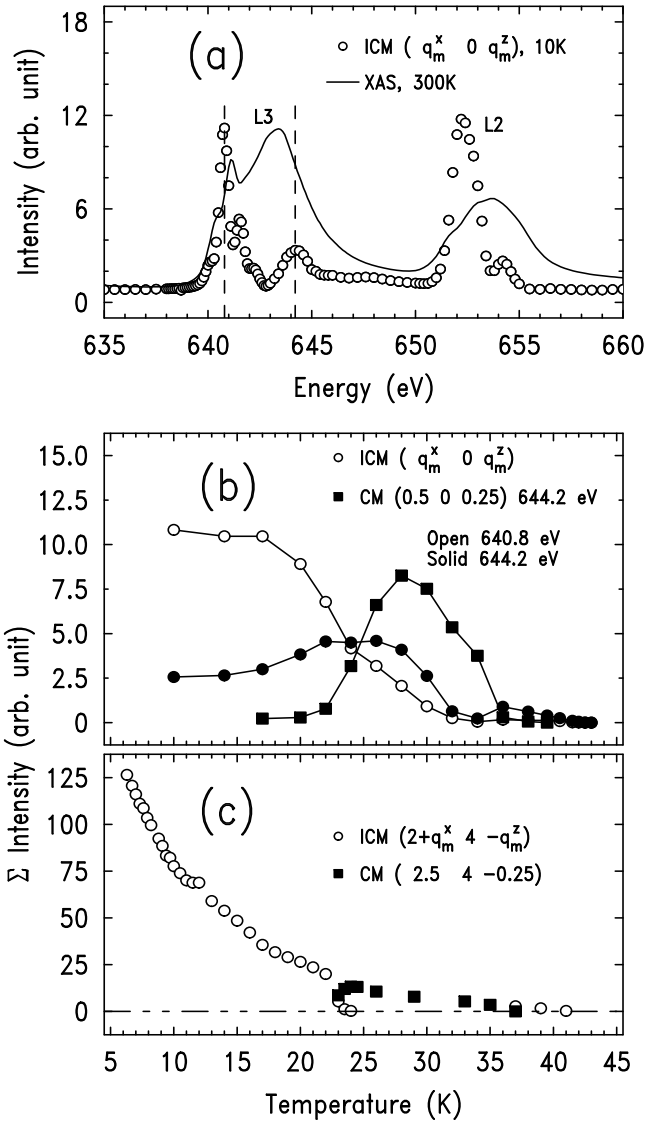

FIG. 4: (a) Energy profiles of the ICM magnetic peaks (circle)and XAS (solid line) around Mn $L_{2,3}$-edges. Vertical broken lines correspond to 640.8 eV and 644.2 eV, respectively. (b) Temperature dependences of the ICM (circle) and the CM (square) magnetic peaks. Open (Solid) symbols denote the data taken E = 640.8 eV (644.2 eV), respectively. (c) Temperature dependences of the ICM (open circle) and the CM (solid square) magnetic peak at Tb L_3-edge.

parallel. Therefore, although the resonances do not have one-to-one correspondences with the magnetic orders of Mn ions, changes in the resonances at magnetic satellites reflect the changes in spin ordering which are periodically modulated with the wave vector $\boldsymbol{q}_m$. Temperature dependences of x-ray intensities at the ICM peak of $\boldsymbol{Q}_m$ = (q_m^x 0 q_m^z) were measured at the two resonances, 640.8 and 644.2 eV. The results are presented in Fig. 4 (b). Data for a CM peak of $\boldsymbol{Q}_m$ = (0.5 0 0.25) at the resonance of 644.2 eV are presented together. It is clear that, above 15 K, intensities of each resonance have different temperature dependences from each other. Though the origin of the anomalous temperature dependences is not understood in detail, it reflects complicated natures of magnetic moments of Mn ions under the frustrated configuration.

Magnetic ordering of Tb^{3+} ions was investigated with resonant x-ray scattering measurements at Tb L_3-edge. Figure 4 (c) shows that ordering temperature of Tb magnetic moments is the same with that of Mn, T_N, which is consistent with neutron scattering results [9]. The modulation wave vector of Tb magnetic order is the same with the values of $\boldsymbol{q}_m$ measured in nonresonant x-ray scattering. Soft x-ray magnetic scattering measurements were also performed at Tb M_5-edge and the result not shown here confirms that observed x-ray intensities in Fig. 4 (c) reflect magnetic order of Tb $4f$ electrons which grows monotonically below T_N.

From the results shown in Fig. 4 (b) and (c), it is clear that there exist multiple magnetic order parameters having the same $\boldsymbol{q}_m$'s but different temperature dependences. The contributing portions of each magnetic order to scattering factors of magnetic satellites are different depending on $\boldsymbol{Q}_m (= \boldsymbol{Q}_{Bragg} + \boldsymbol{q}_m)$, and it results in different temperature dependence for each magnetic peak and its corresponding lattice modulation peak intensities, which explains the temperature dependences presented in Fig. 3.

Since the magnetic orders are located under the spin frustrated geometry, it is reasonable to suppose that phase-slips take place due to competitions between the magnetic orders, as their order parameters grow with different temperature dependences. The discommensuration results in the transition to the LT-ICM phase. Anti-phase domain walls for the phase slips are consistent with the aforementioned long-period CM modulations below T_{c3}. Assuming the model suggested by others [9], atomic displacements are canted antiferroelectric type. Across an anti-phase domain wall, directions of the atomic displacements and the spontaneous polarizations are reversed. Therefore, not only the polarizations from domains separated by the domain wall cancel each other but also x-ray scattering amplitudes for the (3 0 0) Bragg peak are canceled due to the crystal symmetry. Then, only remnants resulting from unequal populations of the domains contribute to P and $I_{(300)}$. Since a density of the domain walls determines $\boldsymbol{q}_m$, temperature dependences of P, $I_{(300)}$ and $\boldsymbol{q}_m$ down to T_{c3} can be explained consistently in terms of CM modulations with the anti-phase domain walls. This indicates that CM modulations are preferred as its low temperature ground state. Then, the low temperature phase seems to have a higher entropy due to the domain walls than the high temperature CM phase, violating the entropy rule. However, due to the geometrical frustration and the presence of multiple magnetic orders many different energy scales can exist. The complicated temperature dependences of the magnetic orders in Fig. 4(c) reflect the presence of the different energy scales. Smaller energy scales become important at low temperatures and induce discommensuration. Upturns of the electrical polarization and $I_{(300)}$ below T_{c3} are attributed to lattice modulations enhanced by increasing Tb magnetic moments, which is consistent with results of others demonstrating couplings between Tb moments and lattices [18, 19, 20].

In summary, we have shown that exchange striction is the driving mechanism for the magnetoelectricity in the material. The same temperature dependences of x-ray intensities at a (3 0 0) forbidden Bragg peak and a lattice modulation peak in the CM FE phase, together with observation of the relation, $\boldsymbol{q}_c = 2\boldsymbol{q}_m$, demonstrate that spontaneous electric polarization is due to atomic displacements driven by the exchange striction of magnetic orders. Resonant x-ray magnetic scattering results confirm the presence of multiple magnetic orders having different temperature dependences. The CM to LT-ICM phase transition is attributed to discommensuration through phase slipping in the competing magnetic orders in the frustrated configurations. Temperature dependences of $\boldsymbol{q}_m$, P and $I_{(300)}$ in the LT-ICM phase are explained in terms of the CM modulations with anti-phase domain walls.

We thank D.J. Huang for the useful discussions. This work was supported by the KOSEF through the eSSC at POSTECH, and by MOHRE through BK-21 program. The experiments at the PLS were supported by the POSTECH Foundation and MOST. Use of the Advanced Photon Source (APS) was supported by the U.S. Department of Energy, Office of Science, Office of Basic Energy Sciences, under Contract No. W-31-109-Eng-38. The Midwest Universities Collaborative Access Team (MUCAT) sector at the APS is supported by the U.S. Department of Energy, Office of Science, Office of Basic Energy Sciences, through the Ames Laboratory under contract No. DE-AC02-07CH11358. Work at Rutgers was supported by NSF-DMR-0520471.

* Electronic address: kibong@postech.ac.kr
† Present address: European Synchrotron Radiation Facil-

ity, BP 220, F-38043 Grenoble Cedex 9, France
[1] M. Kenzelmann *et al.*, Phys. Rev. Lett. **95**, 87206 (2005).
[2] G. Lawes *et al.*, Phys. Rev. Lett. **95**, 087205 (2005).
[3] S. Kobayashi *et al.*, J. Korean Phys. Soc. **46**, 289 (2005).
[4] N. Hur *et al.*, Nature **429**, 392 (2004).
[5] T. Kimura *et al.*, Nature **426**, 55 (2003).
[6] T. Goto *et al.*, Phys. Rev. Lett. **92**, 257201 (2004).
[7] T. Kimura *et al.*, Phys. Rev. B **68**, 060403(R) (2003).
[8] S.-W. Cheong *et al.*, Nature Mater. **6**, 13 (2007).
[9] L. C. Chapon *et al.*, Phys. Rev. Lett. **93** 177402, (2004). G.R. Blake *et al.*, Phys. Rev. B. **71**, 214402 (2005).
[10] I. Kagomiya *et al.*, Ferroelectrics **286**, 167 (2003).
[11] H. Kimura *et al.*, J. Phys. Soc. Jpn. **75**, 113701 (2006).
[12] L. C. Chapon *et al.*, Phys. Rev. Lett. **96**, 097601 (2006).
[13] V. Polyakov *et al.*, Physica B **297**, 208 (2001).
[14] D. Higashiyama *et al.*, Phys. Rev. B **70**, 174405 (2004).
[15] J.-S. Lee, Ph. D. Thesis, POSTECH (2006).
[16] S. Kobayashi *et al.*, J. Phys. Soc. Jpn. **73**, 3439 (2004).
[17] H. Kawano-Furukawa *et al.*, Phys. Rev. B. **65**, 180508 (2002).
[18] S. Y. Haam *et al.*, Ferroelectrics **336**, 153 (2006).
[19] S.-H. Baek *et al.*, Phys. Rev. B **74** 140410(R) (2006).
[20] R. Valdés Aguilar *et al.*, Phys. Rev. B **74**, 184404 (2006).